Hindawi Publishing Corporation
Journal of Nanomaterials
Volume 2016, Article ID 9592189, 8 pages
http://dx.doi.org/10.1155/2016/9592189

Research Article

The Effect of Structural Properties of Cu_2Se/Polyvinylcarbazole Nanocomposites on the Performance of Hybrid Solar Cells

S. Govindraju,[1,2] N. Ntholeng,[1] K. Ranganathan,[1] M. J. Moloto,[3] L. M. Sikhwivhilu,[4] and N. Moloto[1,2]

[1]*Molecular Sciences Institute, School of Chemistry, University of the Witwatersrand, Private Bag 3, Wits 2050, South Africa*
[2]*Materials for Energy Research Group, University of the Witwatersrand, Private Bag 3, Wits 2050, South Africa*
[3]*Department of Chemistry, Vaal University of Technology, Private Bag X021, Vanderbijlpark 1900, South Africa*
[4]*Nanotechnology Innovation Centre, Advanced Materials Division, Mintek, Private Bag X3015, Randburg 2125, South Africa*

Correspondence should be addressed to N. Moloto; nosipho.moloto@wits.ac.za

Received 19 February 2016; Accepted 27 April 2016

Academic Editor: Umakant M. Patil

It has been said that substitution of fullerenes with semiconductor nanocrystals in bulk heterojunction solar cells can potentially increase the power conversion efficiencies (PCE) of these devices far beyond the 10% mark. However new semiconductor nanocrystals other than the potentially toxic CdSe and PbS are necessary. Herein we report on the synthesis of Cu_2Se nanocrystals and their incorporation into polyvinylcarbazole (PVK) to form polymer nanocomposites for use as active layers in hybrid solar cells. Nearly monodispersed 4 nm Cu_2Se nanocrystals were synthesized using the conventional colloidal synthesis. Varying weight % of these nanocrystals was added to PVK to form polymer nanocomposites. The 10% polymer nanocomposite showed retention of the properties of the pure polymer whilst the 50% resulted in a complete breakdown of the polymeric structure as evident from the FTIR, TGA, and SEM. The lack of transport channels in the 50% polymer nanocomposite solar cell resulted in a device with no photoresponse whilst the 10% polymer nanocomposite resulted in a device with an open circuit voltage of 0.50 V, a short circuit current of 7.34 mA/cm^2, and a fill factor of 22.28% resulting in a PCE of 1.02%.

1. Introduction

There has been a constant drive for cost-effective photovoltaics since the fabrication of the first solar cell [1]. A number of technologies have since been developed as alternatives for p-n junction silicon solar cells [2]. Amongst these technologies, organic solar cells offer much promise in reducing the costs. This is due to their compatibility with solution based roll-to-roll manufacturing hence making them applicable in products with thin film and flexible and light weight features. Currently, state-of-the-art bulk heterojunction solar cells involve the use of conductive polymers as donors and fullerenes as acceptors. These devices have achieved power conversion efficiencies (PCE) of just over 10% [3]. However there has been a rather slow growth to the efficiencies due to a number of factors affecting these devices. Amongst these challenges is the low open circuit voltage (V_{OC}) [4]. There are competing arguments as to what factors affect V_{OC}; some researchers attribute V_{OC} to the mere difference of the work functions of the two metal electrodes and others to the morphology of the active layer or the electrochemical potential of the cathode (poly(3,4-ethylenedioxythiophene):poly(styrenesulfonate), PEDOT:PSS) [5–7].

Replacing the fullerenes with inorganic nanocrystals is thought to be one way of circumventing some of the problems [8]. This results in the so-called hybrid solar cells. Although the efficiencies of hybrid solar cells are lagging behind the fullerene based devices, it is theoretically envisaged that these may surpass the efficiencies as a result of their intrinsic properties such as tunable band gaps, high absorption coefficiencies, and high carrier mobility [9]. In addition, it is possible to synthesize nanocrystals with elongated and branched morphologies resulting in desirable exciton dissociation and charge transport properties [10, 11]. A number of studies using CdS and CdSe as the acceptor material have

been conducted due to the established synthetic methods and thorough understanding of the properties of these materials [12, 13]. Additionally, a number of studies have been reported for improving the performance of polymer/CdSe hybrid solar cells such as the varying of the size and shape of the nanocrystals [14, 15], through surface modification of the nanocrystals [16–18] as well as polymer end-group functionalization [19], and thin film nanomorphology control [20].

Herein, we investigate a similar type of material to CdSe; however we replace the toxic cadmium with widely available and nontoxic copper. If one has to think of industrial scale application, copper selenide then becomes a better alternative. Copper selenide is a semiconductor that exists in many crystalline phases including monoclinic, cubic, and hexagonal and can possess various stoichiometric ratios such as CuSe, Cu_2Se, $CuSe_2$, and Cu_2Se_3. It is reported that Cu_xSe_y has a direct and indirect band gap of 2.2 eV and 1.4 eV, respectively [21]. The interest in employing copper selenide stems from its various reported applications such as thin film photovoltaics, optical filters, and dry galvanic cells (as solid electrolytes) [22, 23].

The morphology of the active layer in hybrid solar cells plays an important role; hence a number of efforts to perfect this have been undertaken. Architectures vary from bilayer structures [24] to bulk heterojunctions [25] to nanorods arrays [26]; however common to all is the need to have good interfacial interaction between the donor and the acceptor materials. Nevertheless whilst interfacial interaction is important, it is critical to have a balance between the filler and the host in order to harness the properties of the filler whilst keeping the integrity of the host material. Herein we therefore propose the use of polymer nanocomposites to form bulk heterojunction structures and we study the effect of the filler concentration (Cu_2Se) on the morphology of the conductive polymer, polyvinylcarbazole (PVK). PVK is a hole transport material (with the hole mobility, μ_h, larger than electron mobility, μ_{el}) exhibiting an emission spectrum that, owing to the carbazole groups, covers the whole blue region [27]. We further report on the effect of the different polymer nanocomposites with varying filler concentrations on the performance of hybrid solar cells.

2. Experimental Section

2.1. Materials. Copper(I) chloride, selenium powder, trioctylphosphine (TOP), hexadecylamine (HDA), polyvinyl-9-carbazole (PVK) (MW 1,100,000 $gmol^{-1}$), pyridine, methanol, acetone, isopropanol, and poly(3,4-ethylenedioxythiophene)-poly(styrenesulfonate) were all purchased from Sigma-Aldrich.

2.2. Synthesis of the Cu_2Se Nanocrystals. Cu_2Se nanocrystals were synthesized using a method that we described earlier [28]. In a typical synthesis 0.8 g of CuCl was dissolved in 5 mL of TOP; the solution was stirred for 1 hr at room temperature. 1.0 g of Se powder was dissolved in 5 mL of TOP and the solution was also stirred for 1 hr at room temperature. About 5 g of HDA was heated under N_2 gas to 100°C. Thereafter the TOP-Se solution was added to the HDA and the temperature was increased to 220°C. At 220°C the TOP-CuCl solution was added to the reaction flask and a temperature drop was observed. The temperature was then increased to 220°C and then the timer was started. Aliquots at 2, 4, 6, 8, and 10 min were then taken. The nanocrystals were flocculated by the addition of methanol. The resultant crystals were then washed several times with hot methanol and the powders were collected by centrifugation and they were allowed to dry in air.

2.3. Synthesis of Cu_2Se/PVK Nanocomposites. About 4 nm Cu_2Se nanocrystals were first dispersed in pyridine in order to exchange the long-chained HDA with a shorter pyridine ligand. The nanocrystals were then flocculated from the pyridine solution by the addition of methanol and subsequently washed several times with methanol and dried at room temperature. The dried powders were then dispersed in chloroform. PVK was subsequently also dissolved in the common solvent chloroform. The two chloroform solutions were mixed and allowed to stir for 30 min at 70°C. The resultant composite was flocculated by the addition of methanol and collected through centrifugation. The amount of the nanocrystals was varied (10, 20, 30, and 50 wt.%) to give the desired composition of the nanocomposite.

2.4. Fabrication of the Hybrid Solar Cells. The structure of the devices consisted of the following layers of films: ITO/PEDOT-PSS/Cu_2Se/PVK nanocomposite/aluminium. The substrates were routinely cleaned by sequential ultrasonication in acetone, isopropanol, and deionized water and then dried in air for 20 min. Aqueous PEDOT-PSS dispersions were spin-coated on the substrates and then annealed at 150°C for 30 min forming thin films with a thickness of about 55 nm. The nanocomposite layers (25 mg/mL) were spin-coated at 3000 rpm, dried, and annealed at 150°C for 30 min resulting in a thin film coating of ~200 nm. The top Al contacts were sputtered through a shadow mask to generate an array of patterned electrodes. The Al was deposited by thermal evaporation in high vacuum of better than 5×10^{-5} Pa at a rate of about 0.2 nm/s. The final area of each device was 0.08 cm^2 and was defined by the overlap between the top ITO and bottom Al electrodes.

2.5. Instrumentation. The morphology of the nanoparticles and nanocomposites was determined on Tecnai G^2 TEM Spirit operated at 200 kV. SEM analysis was performed on FEI Nova Nanolab 600 FIB/SEM instrument operating at 30 kV. The samples on a carbon tape were coated by a gold-palladium layer before the analysis. A Brüker Tensor 27 Fourier Transform Infrared Spectrometer was used to analyze the surface functionalities and the type of functional groups present on the materials. Thermogravimetric analysis (TGA) was performed with a Perkin-Elmer STA 6000 using nitrogen as the purge gas and a heating rate of 10°C min^{-1}. The flow rate of the purge gas was kept at 20 mL·min^{-1}. A Varian Cary Eclipse (Cary 50) UV-VIS spectrophotometer was used to carry out the absorption measurements. A Varian Cary Eclipse EL04103870 fluorescence spectrophotometer with a medium PMT voltage at an excitation wavelength of

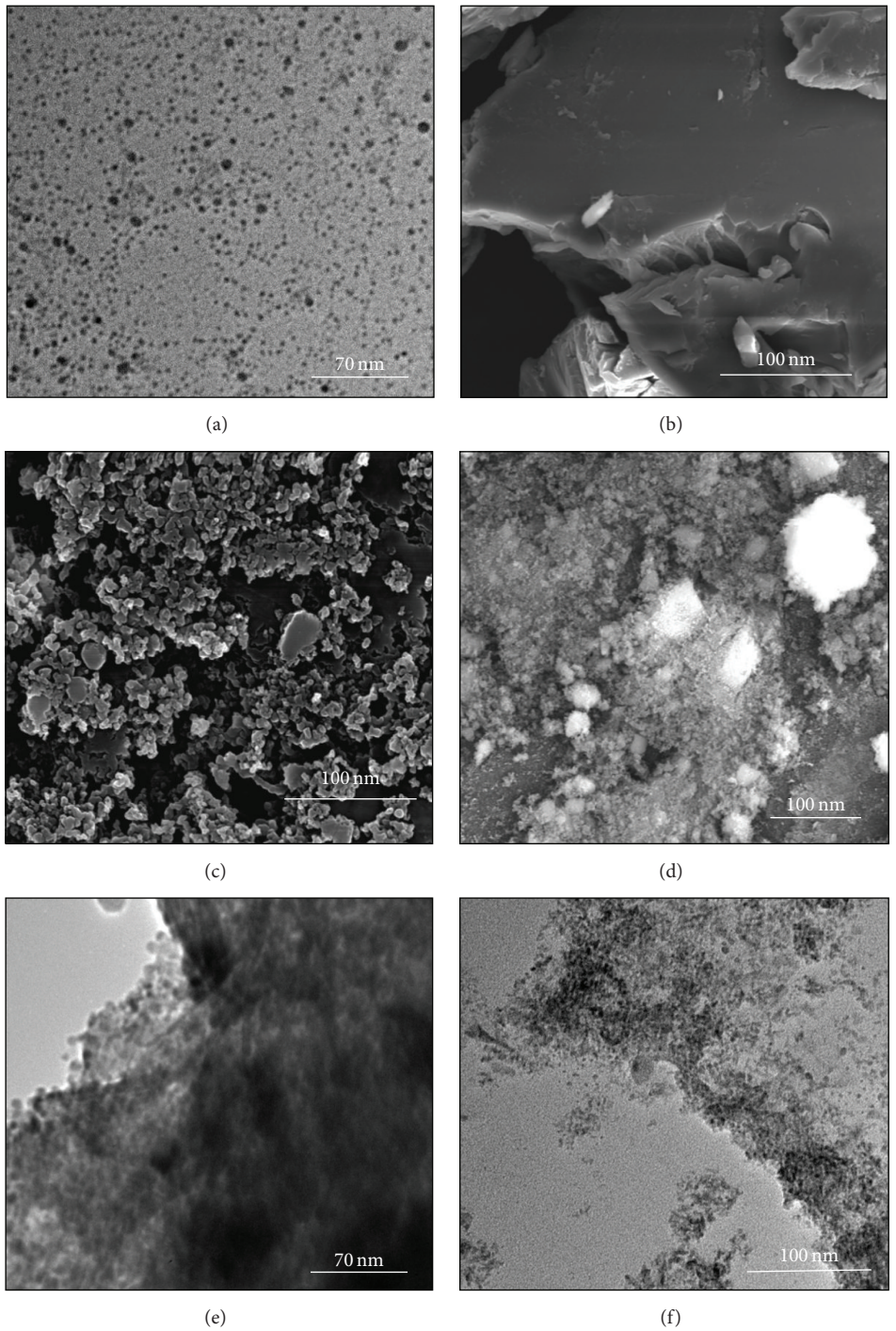

FIGURE 1: (a) TEM micrograph of Cu_2Se nanoparticles, (b) SEM micrograph of PVK, (c) SEM micrograph of 10% Cu_2Se/PVK nanocomposite, (d) SEM micrograph of 50% Cu_2Se/PVK nanocomposite, (e) TEM micrograph of 10% Cu_2Se/PVK nanocomposite, and (f) TEM micrograph of 50% Cu_2Se/PVK nanocomposite.

300 nm was used to measure the photoluminescence (PL) of the samples. For both spectral analyses, the powders were dissolved in chloroform and placed in quartz cuvettes (1 cm path length). The thin film thicknesses were determined by a Filmetrics F20 instrument. The device performances were characterized under AM1.5G 100 mW/cm^2 illumination in a laminar flow cabinet.

3. Results and Discussion

The morphology and the extent of interaction of Cu_2Se with PVK were studied using electron microscopy. Figure 1(a) shows the TEM micrograph of the as-synthesized Cu_2Se nanocrystals. The nanocrystals are spherical with an average size of ~4 nm. The prepared nanocrystals were first stripped

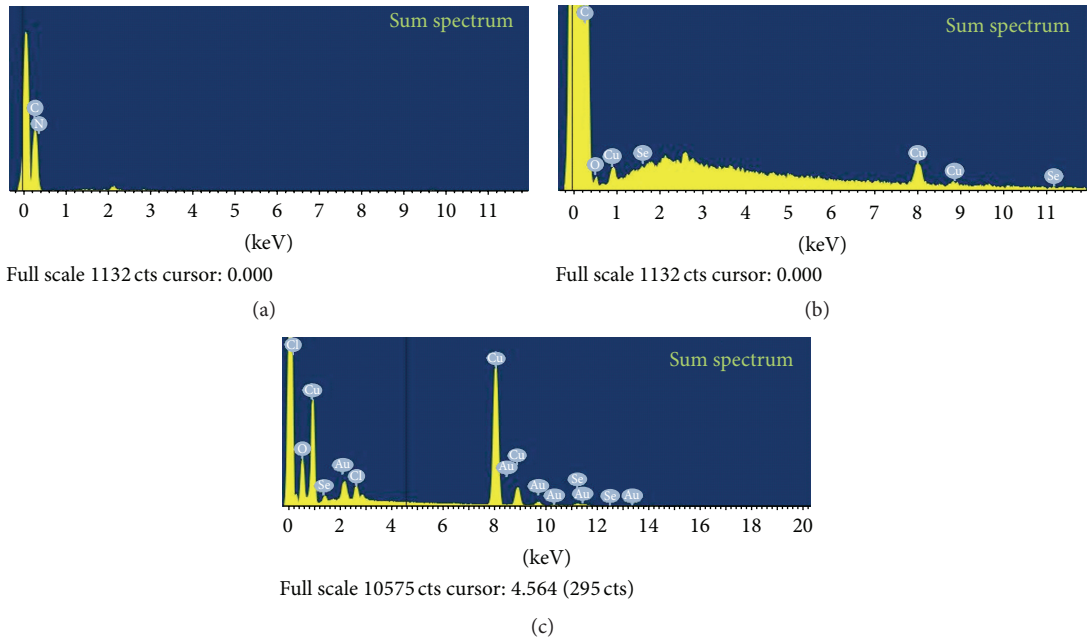

Figure 2: (a) EDX spectrum of PVK, (b) 10% Cu_2Se/PVK nanocomposite, and (c) 50% Cu_2Se/PVK nanocomposite.

off of the long alkyl chained amine HDA, by refluxing in pyridine. Pyridine is known to form weak and reversible bonds with the surface of the nanocrystals [20] and therefore the pyridine molecules can be easily replaced by overwhelming the nanocrystals with polymer molecules. Incremental weight percentages of the nanocrystals to polymer are reported. The 10% addition of Cu_2Se was the minimum amount that showed an appreciative difference between the polymer and the nanocomposites. Meanwhile, 50% was selected as it still preserved some of the features of the polymer yet clearly the nanocrystal features were more dominant. Figures 1(b), 1(c), and 1(d) represent the SEM images of the pristine polymer and 10% and 50% nanocomposites, respectively. The pristine PVK has a smooth morphology consistent with polymers. As 10% by mass of Cu_2Se is added, a change in morphology is observed and the polymer is broken down into particulates in line with the spherical shape of the nanocrystals. This is further exaggerated by the addition of more nanocrystals (50%) where finer spherical particulates are observed. The TEM micrographs of the composites are shown in Figures 1(e) and 1(f). Figure 1(e) shows the presence of greater percentage of the polymer; the more the polymer molecules, the more agglomerated the particles whereas when 50% of the polymer is used whilst some agglomeration is observed the extent is less.

Energy dispersive X-ray spectroscopy (EDX) was done to ascertain the presence of Cu_2Se nanocrystals. The pristine polymer in Figure 2(a) of course shows only the presence of carbon and nitrogen. Figures 2(b) and 2(c) show the presence of copper and selenium with the quantitative amount in (c) larger than in (b) consistent with the 10% and 50% addition.

FTIR spectroscopy can also be a useful tool in determining the extent of the interaction between the polymer and the nanocrystals. Figure 3 shows the FTIR spectra of

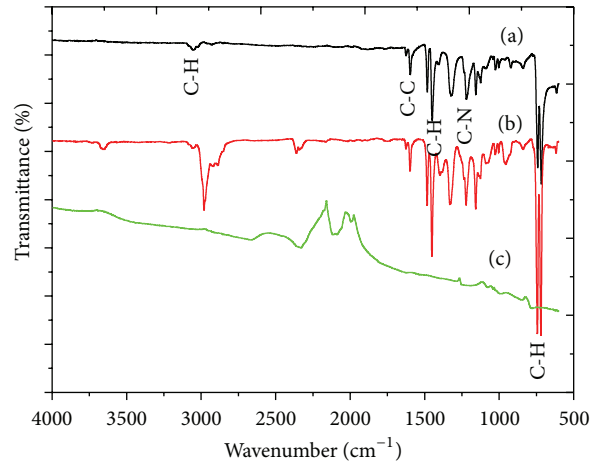

Figure 3: (a) FTIR spectrum of PVK, (b) 10% Cu_2Se/PVK nanocomposite, and (c) 50% Cu_2Se/PVK nanocomposite.

the pure polymer and 10% and 50% nanocomposites. The FTIR spectrum of the 10% nanocomposite is similar to that of the pure PVK; however a slight shift in the C-H stretching frequency from 3060 cm^{-1} for the pure PVK to 2981 cm^{-1} for the nanocomposite as well as the enhancement of the peak is observed. This therefore suggests that the integrity of the polymer is maintained; nevertheless some interaction between the polymer and the nanocrystals is still evident and this bodes well with the morphology observed in the SEM and TEM images. The FTIR spectra of 20% and 30% nanocomposites are shown in the supporting information in Figure S1 in Supplementary Material available online at http://dx.doi.org/10.1155/2016/9592189. Whilst there are appreciable differences between the spectrum of the pure

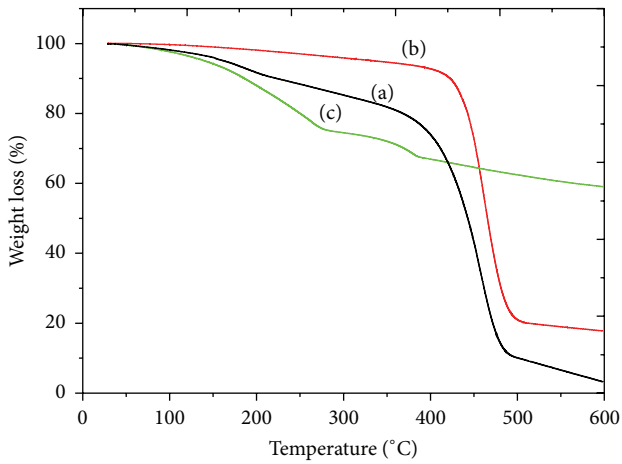

Figure 4: TGA curve of (a) PVK, (b) 10% Cu_2Se/PVK nanocomposite, and (c) 50% Cu_2Se/PVK nanocomposite.

PVK and that of the nanocomposites, the two extreme cases (10% and 50%) were chosen as the difference in properties would be more pronounced. Figure 3(c) depicts the spectrum for the 50% addition of Cu_2Se. The characteristic frequencies for PVK are absent, suggesting a complete breakdown of the polymer structure. This is consistent with the fine particulates observed in the SEM and TEM images.

To further study the structural integrity of the nanocomposites, TGA analysis was performed. Figure 4 shows the TGA curves of the pure polymer and the nanocomposites. Figure 4(a) shows a typical TGA for PVK where the first degradation step is associated with the loss of water and other volatiles that might be present followed by the degradation of the polymer to carbon and then complete decomposition above 450°C. The addition of the nanocrystals results in an improvement of stability of the polymer beyond 600°C and of course the residual remains are attributed to the Cu_2Se nanocrystals. The more the Cu_2Se nanocrystals added (Figure S2 shows the 20 and 30% nanocomposites), the more thermally stable the composite as shown in Figure 4(c).

The optical properties of the HDA-capped Cu_2Se and the nanocomposites are shown in Figure 5. The absorption spectrum of the Cu_2Se nanocrystals shows two well-defined excitonic peaks with the band edge located at 795 nm. The band edge is indicative of an indirect band gap transition and is however blueshifted from the bulk band edge of 886 nm. On the other hand, the photoluminescence spectrum shows a well-defined emission peak with a maximum located at 800 nm and FWHM of 100 nm indicative of a somewhat monodispersed sample. The PVK shows a characteristic absorption peak at the UV region and has a broad emission peak covering the entire UV-Vis region. The optical properties of the 10% Cu_2Se/PVK nanocomposite are similar to those of the pure PVK, a trend that has already been shown. However the photoluminescence spectrum is slightly redshifted from 390 nm for the pure PVK to 397 nm for the composite. The optical properties of the 50% Cu_2Se/PVK are different from the pure PVK with new peaks being observed. These peaks may be attributed to the Cu_2Se nanocrystals.

Table 1: Device properties of the nanocomposites.

Sample	V_{OC} (V)	J_{SC} (mA/cm^2)	FF (%)	η (%)
10% Cu_2Se/PVK	0.50	7.34	22.28	1.02
20% Cu_2Se/PVK	0.50	5.64	22.34	0.79
30% Cu_2Se/PVK	0.50	1.83	22.29	0.25
50% Cu_2Se/PVK	0	0	0	0

The absorption spectrum has peaks in the UV region below 400 nm associated with PVK as well as a shoulder peak depicted in Figure 6 attributed to the Cu_2Se nanocrystals. The peak has an absorption band edge of ~550 nm which is blueshifted from the one observed for the HDA-capped Cu_2Se. This may be as a result of the stripping of the HDA molecules. The photoluminescence spectrum in Figure 5 also has peaks reminiscent of PVK and Cu_2Se nanocrystals. The peaks have however been blueshifted a bit. This is consistent with the observed morphology of the 50% nanocomposite, that is, fine particulates. The emission peak with a maximum at 605 nm shown in Figure 6 is attributed to the nanocrystals and is redshifted from the corresponding absorption band edge in Figure 6. The optical properties presented in Figure 6 suggest that the average particle sizes of the nanocrystals may have reduced due to the treatment with pyridine and the interaction with the polymer.

The synthesized nanocomposites were then tested in a simple device configuration depicted in Figure 7. Due to the energy level offset between the polymer and the nanocrystals, Cu_2Se acts as an electron acceptor and PVK as a hole acceptor. The 50% Cu_2Se/PVK nanocomposite showed no photoresponse whilst the reduction in the wt.% Cu_2Se showed a steady increase in the photoresponse. This could be as a result of the morphology of the nanocomposite. As shown before, too much addition of the nanocrystals breaks down the polymeric structure hence reducing the pathways for the electrons to travel.

The current density-voltage (J-V) curves of the different Cu_2Se/PVK nanocomposite in the dark and under illumination are reported in Figure 7. The device properties for the different nanocomposites are shown in Table 1. The PCE is particularly low when compared to other nanocrystal/polymer hybrid solar cells [9, 20]; however it must be said that the commonly reported work uses different nanocrystals, that is, CdSe or PbS and other polymer combinations. In addition, the reported devices have not yet been optimised; hence there is scope to further increase the efficiency. The FF is particularly low; nonetheless there are a number of strategies that can be used to increase the fill factor, from inverting the architecture of the hybrid solar cell [29] to the introduction of a buffer layer [30] to name a few. V_{OC} and J_{SC} can also be improved, amongst other things, by lowering the band gap of the nanocrystals which can then enable absorption in a longer range; this can be easily achieved by tailoring the size of the nanocrystals. The device with 10 wt.% nanocrystals performed the best with the conversion efficiency of 1.02%. This is attributed to the preservation of the integrity of the polymer thus allowing for electrons to flow easier through the polymeric chains. The 50 wt.% nanocomposite device on

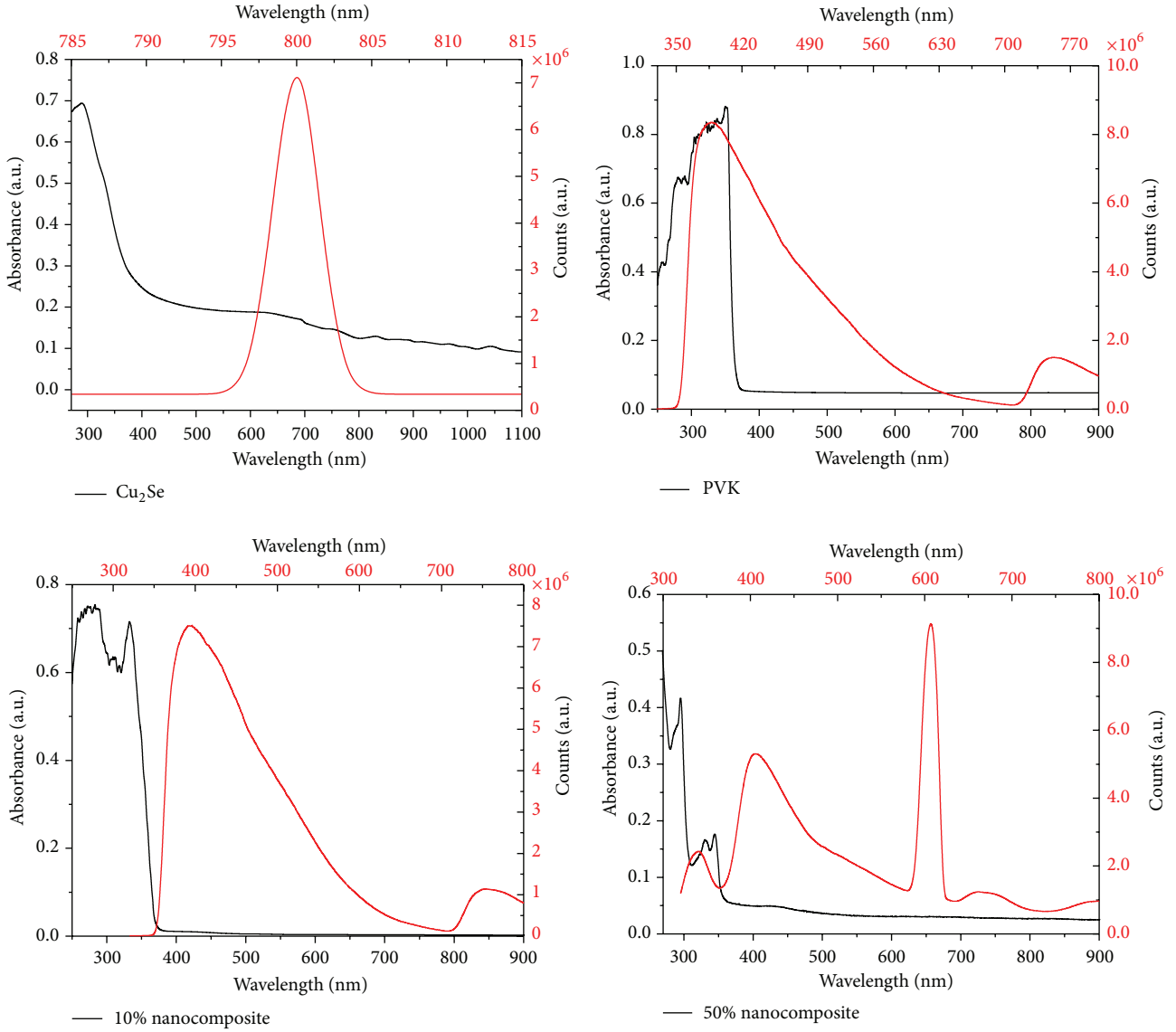

Figure 5: UV-Vis absorption spectra and photoluminescence spectra with excitation at 300 nm for Cu_2Se, PVK, 10% Cu_2Se/PVK nanocomposite, and 50% Cu_2Se/PVK nanocomposite.

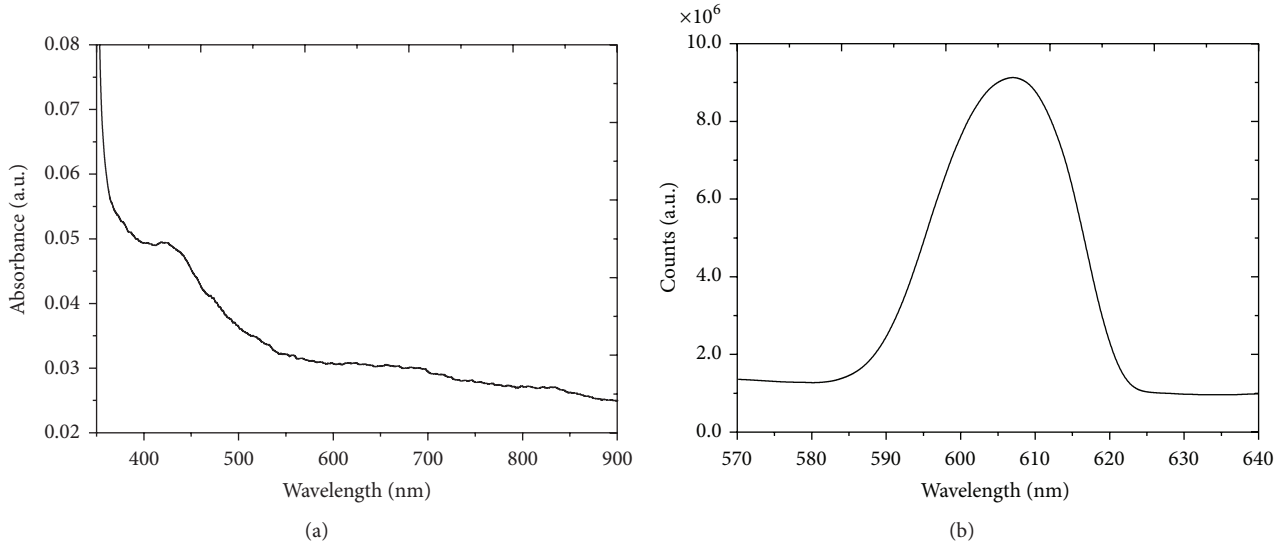

Figure 6: Selected peaks of (a) UV-Vis absorption and (b) photoluminescence spectra of 50% Cu_2Se/PVK nanocomposite.

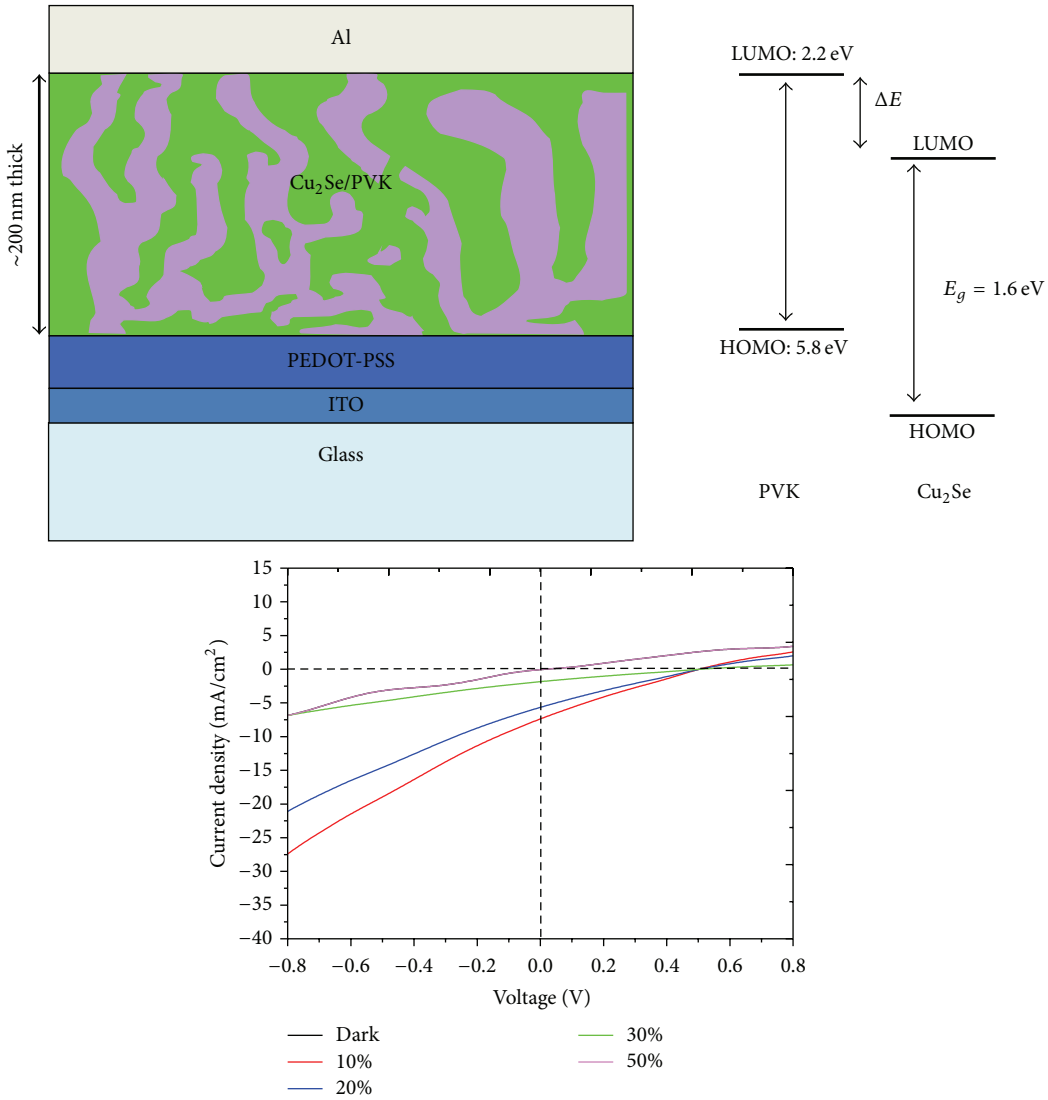

FIGURE 7: Device architecture and J-V curves of the 10, 20, 30, and 50% Cu_2Se/PVK nanocomposites in the dark and under illumination.

the other hand showed no photoresponse, consistent with the breaking down of the polymeric chains as seen in the other results.

4. Conclusion

In conclusion, herein we have shown for the first time that Cu_2Se nanocrystals can be used in hybrid solar cells as an alternative for CdSe and PbS. We have also shown that whilst harnessing the properties of the nanocrystals is important, it is also important to keep the integrity of the polymer as the long chains of polymers play a crucial role in charge transport. Hence we have shown that 10% by weight addition of Cu_2Se improves the properties of PVK and this has resulted in a hybrid solar cell with 0.74% PCE.

Competing Interests

The authors declare that they have no competing interests.

Acknowledgments

The authors would like to thank WITS, MMU, MERG, and NRF for support.

References

[1] D. M. Chapin, C. S. Fuller, and G. L. Pearson, "A new silicon *p-n* junction photocell for converting solar radiation into electrical power," *Journal of Applied Physics*, vol. 25, no. 5, pp. 676–677, 1954.

[2] C. J. Brabec, J. A. Hauch, P. Schilinsky, and C. Waldauf, "Production aspects of organic photovoltaics and their impact on the commercialization of devices," *MRS Bulletin*, vol. 30, no. 1, pp. 50–52, 2005.

[3] Y. Liang, Z. Xu, J. Xia et al., "For the bright future-bulk heterojunction polymer solar cells with power conversion efficiency of 7.4%," *Advanced Materials*, vol. 22, no. 20, pp. E135–E138, 2010.

[4] M. C. Scharber, D. Mühlbacher, M. Koppe et al., "Design rules for donors in bulk-heterojunction solar cells—towards 10%

energy-conversion efficiency," *Advanced Materials*, vol. 18, no. 6, pp. 789–794, 2006.

[5] C. J. Brabec, A. Cravino, D. Meissner et al., "Origin of the open circuit voltage of plastic solar cells," *Advanced Funtional Materials*, vol. 11, no. 5, pp. 374–380, 2001.

[6] J. Liu, Y. Shi, and Y. Yang, "Solvation-induced morphology effects on the performance of polymer-based photovoltaic devices," *Advanced Functional Materials*, vol. 11, no. 6, pp. 420–425, 2001.

[7] H. Frohne, S. E. Shaheen, C. J. Brabec, D. C. Müller, N. S. Sariciftci, and K. Meerholz, "Influence of the anodic work function on the performance of organic solar cells," *ChemPhysChem*, vol. 3, no. 9, pp. 795–799, 2002.

[8] Y. Zhou, M. Eck, C. Veit et al., "Efficiency enhancement for bulk-heterojunction hybrid solar cells based on acid treated CdSe quantum dots and low bandgap polymer PCPDTBT," *Solar Energy Materials and Solar Cells*, vol. 95, no. 4, pp. 1232–1237, 2011.

[9] Y. Zhou, M. Eck, and M. Krüger, "Bulk-heterojunction hybrid solar cells based on colloidal nanocrystals and conjugated polymers," *Energy and Environmental Science*, vol. 3, no. 12, pp. 1851–1864, 2010.

[10] W. U. Huynh, J. J. Dittmer, and A. P. Alivisatos, "Hybrid nanorod-polymer solar cells," *Science*, vol. 295, no. 5564, pp. 2425–2427, 2002.

[11] X. Peng, L. Manna, W. Yang et al., "Shape control of CdSe nanocrystals," *Nature*, vol. 404, no. 6773, pp. 59–61, 2000.

[12] D. V. Talapin, A. L. Rogach, A. Kornowski, M. Haase, and H. Weller, "Highly luminescent monodisperse CdSe and CdSe/ZnS nanocrystals synthesized in a hexadecylamine–trioctylphosphine oxide–trioctylphospine mixture," *Nano Letters*, vol. 1, no. 4, pp. 207–211, 2001.

[13] C. B. Murray, D. J. Norris, and M. G. Bawendi, "Synthesis and characterization of nearly monodisperse CdE (E = S, Se, Te) semiconductor nanocrystallites," *Journal of the American Chemical Society*, vol. 115, no. 19, pp. 8706–8715, 1993.

[14] S. Dayal, M. O. Reese, A. J. Ferguson, D. S. Ginley, G. Rumbles, and N. Kopidakis, "The effect of nanoparticle shape on the photocarrier dynamics and photovoltaic device performance of poly(3-hexylthiophene):CdSe nanoparticle bulk heterojunction solar cells," *Advanced Functional Materials*, vol. 20, no. 16, pp. 2629–2635, 2010.

[15] B. Q. Sun and N. C. Greenham, "Improved efficiency of photovoltaics based on CdSe nanorods and poly(3-hexylthiophene) nanofibers," *Physical Chemistry Chemical Physics*, vol. 8, no. 30, pp. 3557–3560, 2006.

[16] J. S. Owen, J. Park, P.-E. Trudeau, and A. P. Alivisatos, "Reaction chemistry and ligand exchange at cadmium-selenide nanocrystal surfaces," *Journal of the American Chemical Society*, vol. 130, no. 37, pp. 12279–12281, 2008.

[17] J. D. Olson, G. P. Gray, and S. A. Carter, "Optimizing hybrid photovoltaics through annealing and ligand choice," *Solar Energy Materials and Solar Cells*, vol. 93, no. 4, pp. 519–523, 2009.

[18] B. C. Sih and M. O. Wolf, "CdSe nanorods functionalized with thiol-anchored oligothiophenes," *Journal of Physical Chemistry C*, vol. 111, no. 46, pp. 17184–17192, 2007.

[19] J. Liu, T. Tanaka, K. Sivula, A. P. Alivisatos, and J. M. J. Fréchet, "Employing end-functional polythiophene to control the morphology of nanocrystal—polymer composites in hybrid solar cells," *Journal of the American Chemical Society*, vol. 126, no. 21, pp. 6550–6551, 2004.

[20] Y. Wu and G. Zhang, "Performance enhancement of hybrid solar cells through chemical vapor annealing," *Nano Letters*, vol. 10, no. 5, pp. 1628–1631, 2010.

[21] R. Roy, "Accelerating the kinetics of low-temperature inorganic syntheses," *Journal of Solid State Chemistry*, vol. 111, no. 1, pp. 11–17, 1994.

[22] H. W. Hillhouse and M. C. Beard, "Solar cells from colloidal nanocrystals: fundamentals, materials, devices, and economics," *Current Opinion in Colloid and Interface Science*, vol. 14, no. 4, pp. 245–259, 2009.

[23] F. Lin, G.-Q. Bian, Z.-X. Lei, Z.-J. Lu, and J. Dai, "Solvothermal growth and morphology study of Cu_2Se films," *Solid State Sciences*, vol. 11, no. 5, pp. 972–975, 2009.

[24] C. W. Tang, "Two-layer organic photovoltaic cell," *Applied Physics Letters*, vol. 48, no. 2, p. 183, 1986.

[25] H. Hoppe and N. S. Sariciftci, "Organic solar cells: an overview," *Journal of Materials Research*, vol. 19, no. 7, pp. 1924–1945, 2004.

[26] S. Günes, H. Neugebauer, and N. S. Sariciftci, "Conjugated polymer-based organic solar cells," *Chemical Reviews*, vol. 107, no. 4, pp. 1324–1338, 2007.

[27] N. Moloto, N. J. Coville, S. S. Ray, and M. J. Moloto, "Morphological and optical properties of MnS/polyvinylcarbazole hybrid composites," *Physica B: Condensed Matter*, vol. 404, no. 22, pp. 4461–4465, 2009.

[28] S. Govindraju, M. P. Kalenga, M. Airo, M. J. Moloto, L. M. Sikhwivhilu, and N. Moloto, "Size quantization in Cu_2Se nanocrystals," *Optical Materials*, vol. 38, pp. 310–313, 2014.

[29] X. Guo, N. Zhou, S. J. Lou et al., "Polymer solar cells with enhanced fill factors," *Nature Photonics*, vol. 7, no. 10, pp. 825–833, 2013.

[30] C. Platzer-Björkman, P. Zabierowski, J. Pettersson, T. Törndahl, and M. Edoff, "Improved fill factor and open circuit voltage by crystalline selenium at the Cu(In,Ga)Se_2/buffer layer interface in thin film solar cells," *Progress in Photovoltaics: Research and Applications*, vol. 18, no. 4, pp. 249–256, 2010.